INTERNATIONAL JOURNAL OF SATELLITE COMMUNICATIONS AND NETWORKING
Int. J. Satell. Commun. Network. 2010; **00**:1–20
Published online in Wiley InterScience (www.interscience.wiley.com). DOI: 10.1002/sat

Exploiting Cognitive Radios for Reliable Satellite Communications

Mohammad J. Abdel-Rahman[1], Marwan Krunz[1*], and Richard Erwin[2]

[1] *Department of Electrical and Computer Engineering, University of Arizona, Tucson, AZ 85721, USA*
[2] *Air Force Research Laboratory, Kirtland Air Force Base, Kirtland, NM 87117, USA*

SUMMARY

Satellite transmissions are prone to both unintentional and intentional RF interference. Such interference has significant impact on the reliability of packet transmissions. In this paper, we make preliminary steps at exploiting the sensing capabilities of cognitive radios (CRs) for reliable satellite communications. We propose the use of dynamically adjusted frequency hopping (FH) sequences for satellite transmissions. Such sequences are more robust against targeted interference than fixed FH sequences. In our design, the FH sequence is adjusted according to the outcome of out-of-band proactive sensing, carried out by a CR module that resides in the receiver of the satellite link. Our design, called OSDFH (Out-of-band Sensing-based Dynamic Frequency Hopping), is first analyzed using a discrete-time Markov chain (DTMC) framework. The transition probabilities of the DTMC are then used to measure the "channel stability," a metric that reflects the freshness of sensed channel interference. Next, OSDFH is analyzed following a continuous-time Markov chain (CTMC) model, and a numerical procedure for determining the "optimal" total sensing time that minimizes the probability of "black holes" is provided. DTMC is appropriate for systems with continuously adjustable power levels; otherwise, CTMC is the suitable model. We use simulations to study the effects of different system parameters on the performance of our proposed design.

Received . . .

KEY WORDS: Cognitive radio; dynamic frequency hopping; Markov models; out-of-band sensing; satellite communications.

1. INTRODUCTION

Recently, there has been significant interest in spectrum-agile software-defined radios (a.k.a. cognitive radios or CRs) to be used in a variety of military and commercial applications. On the commercial side, such systems provide a much needed solution for improving the spectral efficiency of underutilized portions of the licensed spectrum. On the military side, these systems can facilitate interoperability between different radio platforms and also enable prolonged RF communications in the presence of dynamic fluctuations in channel quality.

In this paper, we make preliminary steps at exploring a novel application of the CR technology for reliable satellite communications (SATCOM). Rather than improving the spectrum utilization (which is typically the goal of CRs), in this paper the CR is used as a means of improving the robustness of SATCOM to interference. Specifically, we exploit the sensing capabilities of

*Correspondence to: Marwan Krunz, Department of Electrical and Computer Engineering, University of Arizona. E-mail: krunz@email.arizona.edu

Contract/grant sponsor: Raytheon, AFRL, and Connection One center (an I/UCRC NSF/industry/university consortium)

Contract/grant sponsor: NSF; contract/grant number: CNS-1016943, CNS-0904681, IIP-0832238

CRs to proactively determine the likelihood of high interference on channels that the transmitter will be hopping to in the near future. Satellite transmissions are prone to both unintentional as well as intentional RF interference, which has significant impact on the reliability of packet transmissions. As a first "line of defense," satellite transmissions often rely on spread spectrum techniques, including frequency hopping (FH) and direct sequence [1]. Examples of satellite systems that employ FH include the Advanced Extremely High Frequency (AEHF) [2] and the Military Strategic and Tactical Relay (MILSTAR) [3] satellite systems. Moreover, the Tracking and Data Relay Satellite System (TDRSS), also called the NASA space network, has a spread spectrum mode, called DG1 mode [4]. In fact, FH is extensively used for military SATCOM in challenged (jamming) environments (see [5]). Traditional application of FH involves hopping according to a fixed, pseudorandom noise (PN) sequence, known only to the communicating parties. Although this approach tends to work well in random interference scenarios, it performs poorly in the presence of persistent interference over certain channels. For example, a smart eavesdropper may (eventually) figure out portions of the FH sequence and may attempt to persistently target certain frequencies in certain time slots. In this paper, we only consider a single bent-pipe satellite link. The consideration of networked satellite systems is left for future work.

One way to address the limitations of a static FH approach is to modify/replace the FH sequence according to channel quality and interference conditions. However, the overhead of doing that on the fly is high, and may not be feasible for real-time implementation. Instead, the approach we advocate in this paper relies on exploiting the spectrum sensing capabilities of CRs for *proactive detection of channel quality*. According to this approach, a CR module is placed in the satellite radio system (for uplink transmissions) or at the receiving ground station (for downlink transmissions). This module monitors frequencies that will be used in the near future for transmission according to the given FH sequence. Depending on the quality/stability of the channel, the CR decides which, if any, of the monitored frequencies exhibit high interference, and hence need to be swapped with better quality and/or more stable frequencies (channel stability will be defined later in Section 5.1). The CR module may also recommend boosting the transmission power over certain frequencies to combat relatively mild forms of interference. The CR may also recommend that the transmitter stays silent in certain time slots. The spectrum sensing results are reported to the transmitter via a feedback channel (e.g., a reverse link, as shown in Figure 1). The feedback channel is a separate frequency channel from the receiver to the transmitter of the satellite link. The feedback channel of the uplink is different from the downlink data channel(s) (similarly, the feedback channel of the downlink is different from the uplink data channel(s)). The feedback channel is used to convey ACK messages in addition to other feedback messages. This channel is assumed to be sufficiently reliable, which can be achieved by using strong error correction code. Feedback messages are small in size, and hence can be piggybacked on the ACK messages from the receiver to the transmitter. The feedback delay is equivalent to one round-trip time (RTT), which is in the order of a few 100s of milliseconds. By focusing on "future" frequencies in the FH sequence, our approach prevents (rather than reacts to) disruptions to ongoing communications.

The remainder of this paper is organized as follows. Section 2 gives an overview of related work. Section 3 introduces our proposed proactive sensing approach. The discrete-time Markov chain (DTMC) model is discussed in Section 4. In Section 5 we discuss the proposed OSDFH (Out-of-band Sensing-based Dynamic Frequency Hopping) protocol. The continuous-time Markov chain (CTMC) model is presented in Section 6. Section 7 provides a numerical procedure for optimizing the total sensing time so as to minimize the probability of "black holes". We evaluate the OSDFH design in Section 8. Finally, Section 9 provides concluding remarks. Table I provides a list of notations used throughout the paper.

2. RELATED WORK

Our work is related to four main research areas, namely, out-of-band sensing, dynamic frequency hopping (DFH), CRs, and satellite communications. Some of the important contributions in out-of-band sensing and DFH include [6–9]. In [6], DFH "communities" were proposed for efficient

DOI: 10.1002/sat

Table I. List of notations.

Notation	Definition
m	Period of the FH sequence
T	Duration of one slot in the FH sequence
f_i	ith frequency channel
F	Number of channels
d_i	Frequency used in the ith slot of the PN code
τ_s	Sensing time
l	$\frac{T}{\tau_s}$
K	Lag parameter
τ_f	Feedback time
h_n	Frequency that is actually used in the ith slot of the FH sequence
P_{nominal}	Nominal power
Y_i	Received power during time slot i
B	One-sided bandwidth of the low-pass signal
u	$\tau_s B$
λ_1 and λ_2	Thresholds for determining channel quality/usability
$P_{\max}$	Maximum allowable transmission power
N_{λ_j}	Level-crossing rate of Y_i at λ_j
π_j	Steady state probability of being in state j
p_{th}	Stability threshold
SINR_{th}	SINR threshold

frequency usage and reliable channel sensing in IEEE 802.22 systems. The key idea in a DFH community is that neighboring WRAN (wireless regional area network) cells form cooperating communities that coordinate their DFH operation. In [7] the hopping mode of the IEEE 802.22 standard was compared with its non-hopping mode. The results show that hopping reduces collisions with primary users and achieves higher throughput, thus providing enhanced QoS for secondary users (SUs). In [8], the use of out-of-band sensing was investigated. Sensing consumes part of the MAC frame that would otherwise be used for data transmission. In [9], a cooperative out-of-band sensing was investigated. The authors used the ATSC TV signal as an incumbent signal, and derived the mis-detection and false-alarm probabilities under a frequency-selective Rayleigh fading channel.

Motivated by the increased demand for satellite multimedia and broadcasting services, several works have recently proposed using CRs to efficiently utilize the satellite bands (see for example [10–13]). In [11] and [13] the authors considered a hybrid satellite-terrestrial system. In [11], it is assumed that one of the two systems (satellite or terrestrial) uses the spectrum of the other system in an opportunistic fashion (i.e., as a secondary system). Considering this spectrum sharing model, the authors in [11] studied the performance of energy-based sensing. In [13] the cognitive satellite terrestrial radios (CSTRs) were proposed for two specific applications of hybrid satellite-terrestrial systems (HSTS): a satellite-UWB (ultra wideband) system for personal area networks (PAN) with short range communication, and a satellite-WRAN system for long range communication. Different cognitive techniques, including underlay, overlay, interweave, and database, were discussed in [10] in the context of SATCOM. Yun et. al. [12] proposed a scheme for overlaying an SU signal over a satellite communication channel, where the transmitter and receiver of the secondary system are optimally selected to minimize the mean square error (MSE) at the output of the secondary receiver.

In contrast to [10–13], in this paper we do not assume a primary/secondary spectrum sharing paradigm. Instead, satellite transmissions are assumed to occur over dedicated spectrum bands. However, we exploit the sensing capability of CRs to improve the reliability of SATCOM in the presence of interference. To the best of our knowledge, OSDFH is the first protocol that employs out-of-band sensing of CRs for proactive adjustment of the FH pattern used over a satellite link.

Prepared using satauth.cls
DOI: 10.1002/sat

3. PROPOSED PROACTIVE SENSING APPROACH

3.1. Overview

In this paper, we consider a bent-pipe satellite link, as shown in Figure 1. Frequency division duplexing (FDD) is used to operate the uplink (ground-to-satellite) and downlink (satellite-to-ground) links. The satellite band is divided into several narrowband channels, which can be used for FH. The typical bandwidth of each of these channels is in the order of tens to hundreds of KHz **(e.g., the channel bandwidths used by the gateway stations in the Orbcomm and Starsys LEO satellite systems vary from 50 KHz to 1 MHz [14]. Another example is the Iridium satellite system where the channel bandwidth is 41.67 KHz [15, 16]).** The transmitting ground station uses FH to communicate with a receiving station via satellite. For the uplink (also, downlink), hopping is done according to a given PN sequence that exhibits a sufficiently large period m. Let T be the duration of one slot (time spent transmitting at a given frequency). We assume that T equals to the transmission duration of one packet. Let f_i denote the ith frequency (channel), $i = 1, \ldots, F$. For any given slot j, let d_j denote the frequency selected for transmission according to the given PN code. For example, if f_3 is used for transmission during slot 1, then $d_1 = f_3$. The satellite and/or receiving ground station are augmented with a CR module that is capable of measuring the quality of any channel. The CR considered in our work is a half-duplex radio with "dual-receive capability," wherein two different RF chains are used for sensing one channel and receiving on another channel simultaneously. This dual-receive capability is readily supported by several radios, e.g., QUALCOMM's RFR6500 radio [17] and Kenwood's TH-D7A Dual-band Handheld transceiver [18]. It does not imply using two transceivers. To maintain low hardware complexity, we assume that the CR module cannot measure the interference over the *operating channel* (one currently used for transmission). Interference measurement is performed using an energy-based detector. The CR module senses only one channel at a time. Let τ_s be the time spent sensing a given channel in the FH sequence (a.k.a. *the sensing time*). Typically, $\tau_s \ll T$; τ_s is usually in the order of tens of milliseconds, whereas T can be in 100s of milliseconds to a few seconds. Because we rely on energy-based detectors, the longer the sensing time, the higher is the sensing accuracy. Without loss of generality, we assume $T = l\tau_s$ for some integer l. We also assume a slowly fading satellite channel where the channel coherence time is in the order of a few hundreds of milliseconds.

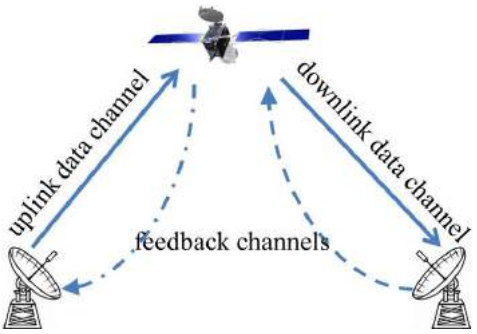

Figure 1. Bent-pipe satellite link with feedback channels.

Consider the uplink data transmission at an arbitrary time slot n (similar treatment applies to the downlink). During that time slot, the transmitting ground station and the receiving satellite will be tuned to frequency d_n. At the same time, the CR module will be sensing channel d_{n+K}, where K (in slots) is called the "lag parameter." If channel d_{n+K} does not satisfy the channel quality requirements described later, the CR module will start sequentially monitoring frequencies d_{n+K+1}, d_{n+K+2}, $\ldots$, $d_{n+K+l-1}$ until it can find a suitable channel to be used for transmission during slot $n + K$ (see Figure 2). Note that in a period T the CR module can sense l channels sequentially. If the CR module cannot find a channel with the desired quality, it instructs the transmitter to stay

DOI: 10.1002/sat

silent during slot $n + K$ (so as not to waste energy). The lag parameter allows for adequate time to report back the outcome of the sensing process. This time is called *the feedback time*, and is denoted by τ_f. It enables the transmitter to adjust its hopping sequence and transmission power accordingly. For typical satellite systems, $\tau_f \sim$ 100s of milliseconds.

Depending on the outcome of the sensing process at time n, the CR may recommend that the transmitter stays silent in slot $n + K$, or to transmit using a recommended channel, denoted by h_{n+K}. This channel h_{n+K} may be the same as d_{n+K} (the channel that was supposed to be used according to the original FH sequence) or it may be a different channel. The transmission is done using a predefined nominal power P_{nominal}, or a power boost may be required. The transmitter criterion will be explained in detail in Section 3.3.

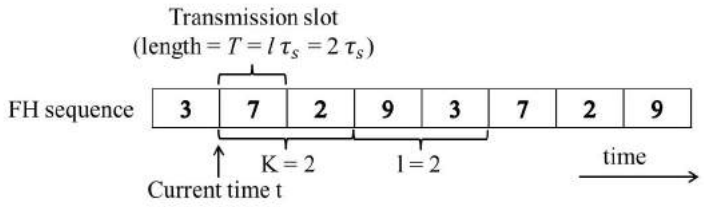

Figure 2. Sensing "future" frequencies (K = 2, l = 2).

3.2. *Decision Criterion at the CR Module*

To measure the quality of the sensed channel, the CR uses two metrics: "channel quality" and "channel stability." This section introduces the first metric. The second metric will be discussed in Section 5.1. The CR module uses the received power to decide whether the channel is usable or not based on a predefined threshold. The received signal at the CR module at time t can be expressed as $R(t) = hI(t) + N(t)$, where $I(t)$ is the received interference signal, $N(t)$ is the noise signal, and h is a binary variable which equals to one if the monitored channel undergoes interference (hypothesis H_1) and zero otherwise (hypothesis H_0). Under hypothesis H_0, the received power (which is considered as the decision statistic) during time slot i is denoted by $Y_i^{(H_0)}$ and is approximately given by [19]:

$$Y_i^{(H_0)} = \frac{1}{2u} \sum_{j=1}^{2u} n_j^2 \tag{1}$$

where $u = \tau_s B$ is the time-bandwidth product, B is the one-sided bandwidth of the low-pass signal, and n_j is a Gaussian noise signal with zero mean and unit variance. It is known that $Y_i^{(H_0)}$ follows a central Chi-Square distribution of $2u$ degrees of freedom, mean one, and variance $1/u$ [19]. Under hypothesis H_1, the received power during slot i, denoted by $Y_i^{(H_1)}$, follows a noncentral Chi-Square distribution of $2u$ degrees of freedom and a non-centrality parameter of 2γ, where γ is the interference-to-noise ratio (INR). Under hypothesis H_1, the mean of $Y_i^{(H_1)}$ is $1 + \gamma/u$ and its variance is $1/u + (2\gamma)/u^2$. Hence, for a given B as τ_s increases the variance of the received power under both hypothesis decreases. The probability density function (pdf) of Y_i can then be written as:

$$f_{Y_i}(y) = \begin{cases} \frac{u^u}{\Gamma(u)} y^{u-1} \exp(-uy), \forall y \geq 0, & \text{under } H_0 \\ u \left(\frac{uy}{\gamma}\right)^{\frac{u-1}{2}} \exp(-uy - \gamma) I_{u-1}\left(2\sqrt{\gamma uy}\right), \forall y \geq 0, & \text{under } H_1 \end{cases} \tag{2}$$

where $\Gamma(\cdot)$ is the Gamma function and $I_v(\cdot)$ is the vth-order modified Bessel function of the first kind. For the rest of the paper, we use Y_i to refer to the received power (decision statistic), whenever there is no particular hypothesis under consideration.

DOI: 10.1002/sat

Consider the sensing outcome (i.e., Y_i) over a given channel. The CR decision criterion can be expressed as follows:

$$\begin{cases} d_i \text{ is clean (usable)}, & \text{if } Y_i < \lambda_1 \\ d_i \text{ requires power boost (usable)}, & \text{if } \lambda_1 < Y_i < \lambda_2 \\ d_i \text{ cannot be used in slot } i \text{ (unusable)}, & \text{if } Y_i > \lambda_2 \end{cases} \tag{3}$$

where λ_1 and λ_2 are thresholds to be determined (see Figure 3). If the sensed channel cannot be used during a given future slot i, the CR module sequentially checks the subsequent l channels (according to the given PN sequence) until it finds a channel that can be swapped with the channel currently assigned to slot i. If all the l channels cannot be used during slot i, the CR module recommends the transmitter to stay silent during that slot.

3.3. Decision Criterion at the Transmitter

During time slot i, the transmitter may communicate over channel d_i or it may swap this channel with one of the channels $d_{i+1}, d_{i+2}, \ldots, d_{i+l-1}$. In either case, the transmitter will either use power level P_{nominal} or it may boost its transmission power, up to a maximum value $P_{\max}$. If the CR module cannot find a channel that satisfies the channel quality requirements, described in Section 5, then it will recommend that the transmitter stays silent during slot i. Figure 3 shows the relation between the received noise-plus-interference power over a given channel (as measured by the CR module) at a given time, and the required transmission power (by the transmitter of the satellite link) over this channel after KT seconds in order to have a correct reception (i.e., the SINR at the receiver of the satellite link exceeds a certain threshold). The values of the power boost (when $\lambda_1 < Y_i < \lambda_2$) and h_i (in case of channel swapping) are fed back to the transmitter. The transmitter indicates its transmission power in its messages to the receiver. This enables the receiver to determine the channel gain between the transmitter and itself, after measuring the received power. For correct reception, the receiver requires the signal-to-interference-plus-noise (SINR) ratio to be greater than a certain threshold. Given the current SINR value, the receiver calculates the required SINR boost, which translates into a required boost on the transmission power. This power boost is fed back to the transmitter. Recall that $h_i \in \{d_i, \ldots, d_{i+l-1}\}$ is the channel that will actually be used for transmission during slot i. In the subsequent analysis, we say that channel h_i is in state 1 if $Y_i < \lambda_1$, in state 2 if $\lambda_1 < Y_i < \lambda_2$, and in state 3 otherwise.

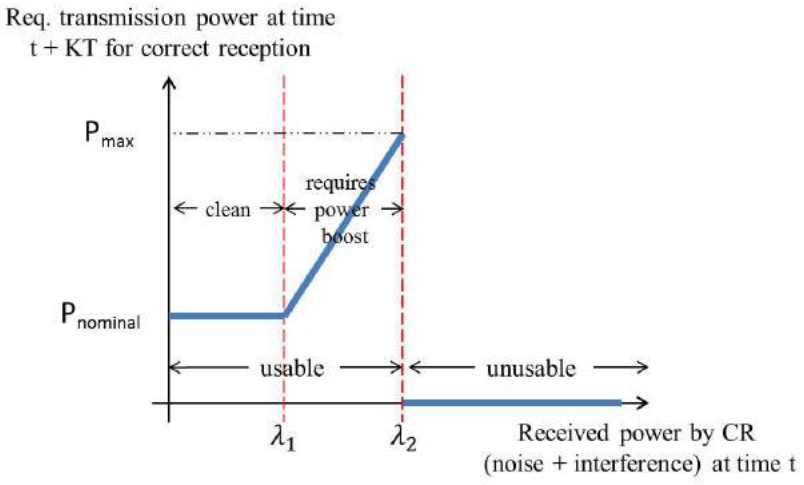

Figure 3. Required transmission power by the transmitter of the satellite link vs. the received noise-plus-interference power at the CR module.

DOI: 10.1002/sat

4. DTMC CHANNEL MODEL

In this section, we characterize channel dynamics using DTMC. Using this model, we later assess the stability of the monitored channel. According to this model, the received power Y_i is approximated by a discrete-time Markov process with time slot equals to T. DTMCs have been used to approximate the dynamics of wireless channels, including satellite channels [20]. In our DTMC model, the range of Y_i is divided into three regions: $R_1 \stackrel{\text{def}}{=} \{Y_i : 0 \leq Y_i \leq \lambda_1\}$, $R_2 \stackrel{\text{def}}{=} \{Y_i : \lambda_1 \leq Y_i \leq \lambda_2\}$, and $R_3 \stackrel{\text{def}}{=} \{Y_i : Y_i \geq \lambda_2\}$. The boundaries of the three regions are parameters to be computed. In the literature, researchers have used DTMC models to characterize the channel, but without allowing for transitions between non-adjacent states. Therefore, they assume that once Y_i is in a given state, it stays in it for at least T seconds, and can only transition to the same state or adjacent states in the next T seconds. Let us denote the transition probability from state k to state j by $p_{k,j}, k, j = 1, 2, 3$. Then, $p_{k,j}$ can be expressed as:

$$p_{k,j} = \begin{cases} \frac{N_{\lambda_k} T}{\pi_k}, & \text{if } |j-k| \leq 1 \text{ and } j > k \\ \frac{N_{\lambda_j} T}{\pi_k}, & \text{if } |j-k| \leq 1 \text{ and } j < k \\ 1 - \sum_{i \neq k} p_{k,i}, & \text{if } j = k \\ 0, & \text{if } |j-k| > 1 \end{cases} \tag{4}$$

where $N_{\lambda_j}, j = 1, 2$, is the *level-crossing rate* (LCR) of Y_i at λ_j (the rate at which Y_i crosses level λ_j in the upward/downward direction) and π_j, $j = 1, 2, 3$, is the steady-state probability of being in state j. Note that $p_{k,j}$ can be expressed as $N_{\lambda_{\min\{k,j\}}} T/\pi_k$ if $|j-k| \leq 1$, and the first two cases of (4) can be combined into one case. Denote the time derivative of Y_i by $\dot{Y}_i$. Then, N_{λ_j} is given by [21]:

$$N_{\lambda_j} = \int_{y \geq 0} \dot{y} f_{Y_i, \dot{Y}_i}(\lambda_j, \dot{y}) d\dot{y} = \Pr[H_0 \text{ occurs}] \cdot N_{\lambda_j | H_0} + \Pr[H_1 \text{ occurs}] \cdot N_{\lambda_j | H_1} \tag{5}$$

where $f_{Y_i, \dot{Y}_i}(\lambda_j, \dot{y})$ is the joint pdf of Y_i and $\dot{Y}_i$, and $N_{\lambda_j | H_0}$ and $N_{\lambda_j | H_1}$ are the conditional values of N_{λ_j} when H_0 and H_1 occur, respectively. $N_{\lambda_j | H_0}$ and $N_{\lambda_j | H_1}$ are given by [22]:

$$N_{\lambda_j | H_0} = \frac{2u^2}{\Gamma(u)} (\lambda_j u)^{u-1} \exp(-\lambda_j u) \tag{6}$$

$$N_{\lambda_j | H_1} = 2u \left(\sqrt{2\gamma} \lambda_j u\right)^{u-1} \exp(-\lambda_j u - 2\gamma) \sum_{l \geq 0} \frac{(\lambda_j u \gamma)^l}{l! \Gamma(u+1)} \sum_{k \geq 0} \frac{\gamma^k}{k! \Gamma(u+k)} \int_{t \geq 0} t^{u+k} \exp(-t) dt \tag{7}$$

where $\int_{t \geq 0} t^{u+k} \exp(-t) dt$ is the incomplete Gamma function of the first kind. The steady-state probability of being in state j is given by $\pi_j = \Pr\{Y_i \in R_j\} = \Pr\{\lambda_{j-1} \leq Y_i < \lambda_j\}$, which can be expressed as:

$$\pi_j = \int_{\lambda_{j-1}}^{\lambda_j} f_{Y_i}(y) dy = \Pr[H_0 \text{ occurs}] \cdot \pi_{j|H_0} + \Pr[H_1 \text{ occurs}] \cdot \pi_{j|H_1}, j = 1, 2, 3 \tag{8}$$

where $\pi_{j|H_0}$ and $\pi_{j|H_1}$ are given by:

$$\pi_{j|H_0} = 2u \left\{ e^{-\lambda_j u} \sum_{k=0}^{u-1} \frac{1}{k!} (\lambda_j u) - e^{-\lambda_{j-1} u} \sum_{k=0}^{u-1} \frac{1}{k!} (\lambda_{j-1} u) \right\}, j = 1, 2, 3 \tag{9}$$

$$\pi_{j|H_1} = 2u \left\{ Q_u\left(\sqrt{2\gamma}, \sqrt{2u\lambda_{j-1}}\right) - Q_u\left(\sqrt{2\gamma}, \sqrt{2u\lambda_j}\right) \right\}, j = 1, 2, 3 \tag{10}$$

where Q_u is the generalized Marcum's Q function [23].

DOI: 10.1002/sat

In contrast to GEO satellite systems where the channel quality is slowly varying, the channel quality in LEO satellite systems changes rapidly with time (see, for example, [24] and references therein). To capture fast varying channels, we here generalize the DTMC model in [25] [26] to allow transitions between non-adjacent states. In [25] [26], the authors require $p_{k,j} = 0$ for $|j-k| > 1$. In order to remove such a constraint, we aggregate states $k, k+1, \ldots, j-1$ as a new state k' (without loss of generality, assume that $j > k$). Thereby, the transition probability between those two neighboring states is

$$p_{k',j} = \frac{N_{\lambda_{j-1}} T}{\pi_{k'}}, \quad \pi_{k'} = \sum_{i=k}^{j-1} \pi_i. \tag{11}$$

On the other hand, given the initial aggregate state k', the probability that the refined initial state is k is $\pi_k/\pi_{k'}$. Combining the above results, we have

$$p_{k,j} = p_{k',j} \frac{\pi_k}{\pi_{k'}} = \frac{N_{\lambda_{j-1}} T}{\sum_{i=k}^{j-1} \pi_i} \frac{\pi_k}{\sum_{i=k}^{j-1} \pi_i}. \tag{12}$$

Similarly, if $j < k$, then

$$p_{k,j} = \frac{N_{\lambda_j} T}{\sum_{i=j+1}^{k} \pi_i} \frac{\pi_k}{\sum_{i=j+1}^{k} \pi_i}. \tag{13}$$

Combining (4), (12), and (13), $p_{k,j}$, $k, j = 1, 2, 3$ can be expressed as:

$$p_{k,j} = \begin{cases} \frac{N_{\lambda_{j-1}} T}{\sum_{i=k}^{j-1} \pi_i} \frac{\pi_k}{\sum_{i=k}^{j-1} \pi_i}, & \text{if } j \geq k+1 \\ \frac{N_{\lambda_j} T}{\sum_{i=j+1}^{k} \pi_i} \frac{\pi_k}{\sum_{i=j+1}^{k} \pi_i}, & \text{if } j \leq k-1 \\ 1 - \sum_{i \neq k} p_{k,i}, & \text{if } j = k. \end{cases} \tag{14}$$

Let $P = [p_{i,j}]$ be the transition probability matrix, and let P^k be the k-step transition probability matrix. The (i,j) entry of P^k is denoted by $p_{i,j}^{(k)}$. Let $\pi = (\pi_1 \ \pi_2 \ \pi_3)$ be the steady-state distribution.

Selection Criterion of λ_1 and λ_2: The range of each state needs to be large enough to cover the variations in Y_i during a packet time, so that for most of the time a received packet completely falls in one state. On the other hand, the range of each state cannot be made too large; otherwise the time spent in a state is much larger than the packet duration. In this case, the variations in Y_i during a packet time are much smaller than the variations in Y_i during the state interval, and different packets falling in the same state may experience quite different qualities. From the above discussion, it is clear that the average duration of a state is a critical parameter in our DTMC model. We define $\bar{\tau_j}$ as the average time spent in state j. This $\bar{\tau_j}$ represents the ratio of the total time the received signal remains between λ_{j-1} and λ_j and the total number of such time segments, both measured over a long time interval τ. Let τ_i be the duration of each time segment when the signal remains between λ_{j-1} and λ_j. Then, $\bar{\tau_j}$ can be expressed as [26]:

$$\bar{\tau_j} = \frac{\sum \tau_i}{(N_{\lambda_{j-1}} + N_{\lambda_j})\tau} = \frac{\pi_j}{N_{\lambda_{j-1}} + N_{\lambda_j}}. \tag{15}$$

We require that

$$\bar{\tau_j} = c_j T, \quad j = 1, 2, 3 \tag{16}$$

where c_j is a constant greater than 1. As discussed earlier, c_j needs to be made large enough so that for most of the time a received packet completely falls in one state. On the other hand, it cannot be too large, so as to ensure that all packets falling in the same state experience approximately the same quality. From (5), (8), (15), and (16), c_j, $j = 1, 2, 3$, can be expressed as:

$$c_j = \frac{\Gamma(u)}{uT} \frac{e^{-\lambda_{j-1}u} \sum_{k=0}^{u-1} \frac{(\lambda_{j-1}u)^k}{k!} - e^{-\lambda_j u} \sum_{k=0}^{u-1} \frac{(\lambda_j u)^k}{k!}}{(\lambda_{j-1}u)^{u-1} e^{-\lambda_{j-1}u} + (\lambda_j u)^{u-1} e^{-\lambda_j u}}. \tag{17}$$

DOI: 10.1002/sat

For given values of λ_1 and λ_2, we can obtain the corresponding c_j values. Our purpose is to find λ_1 and λ_2 with the requirement that the time durations c_j (in number of packets) are within a reasonable range. If we set $c_j, j = 1, 2, 3$, in (17) to some given values, we will have three equations with two unknowns (λ_1 and λ_2). We address this overdetermined system of equations by requiring that $c_1 = c_2 = c_3 = c$ for some constant c (to be determined). Thus, each state has the same average time duration. The equations in (17) now contain three unknowns: λ_1, λ_2, and c.

5. OSDFH PROTOCOL

Following the DTMC channel model, in this section we first introduce the channel stability criterion that the CR module uses to determine if a sensed channel is to be kept or not. We then explain the OSDFH protocol. The specification of various parameters used in this protocol will be discussed in Sections 5.3, 5.4, and 5.5.

5.1. Stability Condition

We say that a channel is stable if with a given probability p_{th}, its quality is not expected to deteriorate before completing the scheduled data transmission on that channel. More specifically, assume that we are currently in slot n and we want to select a channel to be used after K time slots. Then, the stability condition for channel d_{n+K} is

$$p_{i,i}^{(v)} + p_{i,i-1}^{(v)} > p_{th} \tag{18}$$

where $v \stackrel{\text{def}}{=} \left\lceil \frac{KT+T_{data}-x\tau_s}{T} \right\rceil$; T_{data} is the duration of the data transmission, $x\tau_s$ is the total time spent in sensing before finding channel d_{n+K}, and i is the current state of channel d_{n+K}. In the above condition, the values of i that are of interest are 1 and 2, because if the channel is in state 3, then it is unusable and there is no need to check its stability (as we will explain later in Section 5.2).

5.2. Proactive Sensing and Channel Selection Algorithm

In this section, we propose an algorithm for searching for a usable and stable channel, and for adjusting the FH sequence based on channel quality and stability. Our sensing and reporting algorithm can be executed in two steps. First, we search for a usable channel (i.e., channel in states 1 or 2). Second, we test the stability of this usable channel. If the channel is stable, the receiver feeds the channel index along with its state back to the transmitter. Otherwise, the CR module at the receiver searches for another usable channel. The details of these two steps are explained next.

Step 1: Suppose that we are currently in slot n. Then, the CR module will be sensing channel d_{n+K}. If this channel is usable, then step 2 is executed to test its stability. Otherwise, the CR module starts sequentially sensing channels $d_{n+K+1}, d_{n+K+2}, \ldots, d_{n+K+l-1}$ until a usable channel is found. If the CR module can find a usable channel from the $l-1$ channels that follow channel d_{n+K}, then step 2 is executed to test the stability of the selected channel. Otherwise, the CR module informs the transmitter that no usable channel is available, and accordingly the transmitter stays silent during slot $n+K$.

Step 2: If the selected usable channel satisfies the stability condition defined in Section 5.1, then the receiver feeds the index of this channel (frequency) along with its state back to the transmitter. If all the usable channels are unstable, the CR module recommends the transmitter to stay silent during slot $n+K$.

A pseudo-code of the sensing and reporting algorithm is shown in Algorithm 1.

5.3. Determining the Sensing Period

Increasing τ_s decreases the variance of Y_i, thus reducing the uncertainty in the sensing outcome. Let x_r be the rth percentile of Y_i. We select τ_s such that x_r is less than or equal to a predefined value μ.

DOI: 10.1002/sat

Algorithm 1 Out-of-band sensing based DFH

Input: l, T, T_{data}, τ_f, τ_s, λ_1, λ_2, K, and p_{th}
For every time slot T**:**
Step 1: Search for a usable channel
Sense channel d_{n+K}
if state (d_{n+K}) == 3 **then**
  for $x = 1 : l-1$ **do**
    if state $(d_{n+K+x}) < 3$ **then**
      Go to **Step 2** with x and d_{n+K+x}
    end if
  end for
  if no useful usable channel is found **then**
    Inform the transmitter to stay silent
  end if
else
  Go to **Step 2** with d_{n+K}
end if
Step 2: Search for a stable channel
if the usable channel is unstable **then**
  if $x < l-1$ **then**
    Go to **Step 1** to find a usable channel
    if $\exists$ a usable channel d_{n+K+x} for some $x < l-1$ **then**
      Go to **Step 2** with d_{n+K+x}
    else
      Inform the transmitter to stay silent
    end if
  else
    Inform the transmitter to stay silent
  end if
else
  Send the channel index along with its state to the transmitter
end if

The relation between x_r and τ_s can be expressed as:

$$F_{Y_i}(x_r) = \Pr[Y_i \leq x_r] = \Pr[Y_i \leq x_r | H_0] \Pr[H_0 \text{ occurs}] + \Pr[Y_i \leq x_r | H_1] \Pr[H_1 \text{ occurs}] = r. \tag{19}$$

Recall from Section 3.2 that $u = \tau_s B$.

5.4. *Computing* $P_{\max}$ *and* P_{nominal}

To compute $P_{\max}$ and P_{nominal}, we need to consider the SINR, which in the context of satellite communications is referred to as the carrier-to-noise ratio $\left[\frac{C}{N}\right]$. This $\left[\frac{C}{N}\right]$ is expressed in dB as [27, Section 12.6]:

$$\left[\frac{C}{N}\right] = [P_T] + [G_T] + [G_R] - [\text{Losses}] - [P_N] \tag{20}$$

where $[P_T]$ and $[P_N]$ are the transmitted power and the noise-plus-interference power, respectively; $[G_T]$ and $[G_R]$ are the transmitter and the receiver antenna gains, respectively; and $[\text{Losses}]$ are the losses experienced by the signal while propagating in the wireless channel.

$P_{\max}$ is computed by setting $\left[\frac{C}{N}\right]$ to SINR_{th} (the minimum required SINR for the receiver to correctly receive the transmitted signal) and $[P_N]$ to λ_2, both in dB. Then, the corresponding $[P_T]$ is the value of $P_{\max}$. Similarly, P_{nominal} is computed by setting $\left[\frac{C}{N}\right]$ to SINR_{th} and $[P_N]$ to λ_1 in dB. The corresponding $[P_T]$ is the value of P_{nominal}.

5.5. *Selecting the Lag Parameter* K

We select K to be the smallest value that allows the CR module to sense and send its report back to the transmitter in a timely manner. Note that increasing K will decrease the freshness of the sensing outcome (recall that the maximum sensing duration $l\tau_s = T$ is independent of K). Accordingly, we

DOI: 10.1002/sat

set K as:

$$K = \left\lceil \frac{T + \tau_f}{T} \right\rceil = 1 + \left\lceil \frac{\tau_f}{T} \right\rceil . \tag{21}$$

6. CTMC CHANNEL MODEL

Recall that in the DTMC model, λ_1 and λ_2 are obtained by solving the three equations in (17), so they are fixed. The specific selection of λ_1, λ_2, and SINR_{th} values results in specific P_{nominal} and $P_{\max}$ values, as obtained from (20). Therefore, the DTMC model is applicable only when the satellite system can continuously adjust its power according to (20). Alternatively, in this section, we propose a more involved model, in which P_{nominal} and $P_{\max}$ are considered as input parameters. This model is also well-suited for fast varying channels, where channel quality may change continuously with time. In the CTMC model, the range of Y_i is divided into three regions: $R_1 \stackrel{\text{def}}{=} \{Y_i : 0 \le Y_i \le \lambda_1\}$, $R_2 \stackrel{\text{def}}{=} \{Y_i : \lambda_1 \le Y_i \le \lambda_2\}$, and $R_3 \stackrel{\text{def}}{=} \{Y_i : Y_i \ge \lambda_2\}$. Let $S = \{1, 2, 3\}$ denote the state space. For any x and $y \in S$, $x \ne y$, we assign a nonnegative number $\alpha(x, y)$ that represents the rate at which the Markov chain (MC) changes from state x to state y. Let $\rho(x)$ denote the total rate at which the MC leaves state x, i.e., $\rho(x) = \sum_{y \ne x} \alpha(x, y)$. Let A be the infinitesimal generator matrix of the MC; the (x, y) entry of A equals to $\alpha(x, y)$ if $x \ne y$, and equals to $-\rho(x)$ if $x = y$. Let Q_t be the matrix whose (x, y) entry, $q_t(x, y)$, is the probability that the channel transitions from state x to state y in t seconds, $t > 0$. Then, it is known that [28]:

$$Q_t = e^{tA}. \tag{22}$$

Without loss of generality, we assume that the channel **can transit** to adjacent states only (i.e., $\alpha(x, y) = 0$ for $|x - y| > 1$). In other words, the CTMC is a birth-and-death process. The state diagram of the proposed CTMC model is shown in Figure 4.

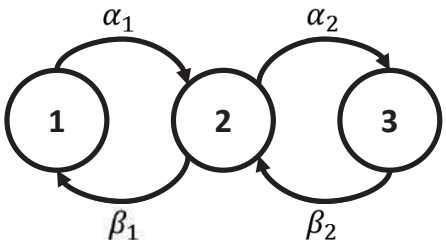

Figure 4. Wireless channel modeled as a three-state continuous-time Markov process.

CTMC models have been previously used to characterize wireless channels [25] [26] [29], and techniques have been proposed to determine the parameters of the MC based on LCR analysis [30] [31]. The LCR at level λ_j, $N_{\lambda_j}, j = 1, 2$, and the corresponding steady-state distribution, $\pi_j, j = 1, 2, 3$, are given by (5) and (8), respectively.

Next, we determine the parameters of the generator matrix A based on the stationary distribution of the system and the level-crossing rates. To simplify the notation, we let $\alpha(1, 2) = \alpha_1, \alpha(2, 1) = \beta_1, \alpha(2, 3) = \alpha_2$, and $\alpha(3, 2) = \beta_2$. Our proposed three-state birth-and-death process is positive recurrent, and has an invariant probability distribution π_j, given by:

$$\pi_j = \frac{\alpha_1 \dots \alpha_{j-1}}{\beta_1 \dots \beta_{j-1}} b^{-1}, \quad j = 1, 2, 3 \tag{23}$$

where π_1 is equal to b^{-1} by convention, and b is given by:

$$b \triangleq \sum_{j=1}^{3} \frac{\alpha_1 \dots \alpha_{j-1}}{\beta_1 \dots \beta_{j-1}} = 1 + \frac{\alpha_1}{\beta_1} + \frac{\alpha_1 \alpha_2}{\beta_1 \beta_2}. \tag{24}$$

DOI: 10.1002/sat

Therefore,

$$\pi_1 = b^{-1} \tag{25}$$
$$\pi_2 = \frac{\alpha_1}{\beta_1} b^{-1} \tag{26}$$
$$\pi_3 = \frac{\alpha_1 \alpha_2}{\beta_1 \beta_2} b^{-1}. \tag{27}$$

Hence, the stationary probabilities are given by:

$$\pi_1 = \frac{\beta_1 \beta_2}{\beta_1 \beta_2 + \alpha_1 \alpha_2 + \alpha_1 \beta_2} \tag{28}$$
$$\pi_2 = \frac{\alpha_1 \beta_2}{\beta_1 \beta_2 + \alpha_1 \alpha_2 + \alpha_1 \beta_2} \tag{29}$$
$$\pi_3 = \frac{\alpha_1 \alpha_2}{\beta_1 \beta_2 + \alpha_1 \alpha_2 + \alpha_1 \beta_2}. \tag{30}$$

The additional relations necessary to uniquely determine A are provided by the LCRs. From [30] [31] [32], $N_{\lambda_j}, j = 1, 2$, can be expressed in terms of α_1, β_1, α_2, and β_2 as:

$$N_{\lambda_1} = \frac{\alpha_1 \beta_1 \beta_2}{\beta_1 \beta_2 + \alpha_1 \alpha_2 + \alpha_1 \beta_2} \tag{31}$$
$$N_{\lambda_2} = \frac{\alpha_1 \alpha_2 \beta_2}{\beta_1 \beta_2 + \alpha_1 \alpha_2 + \alpha_1 \beta_2}. \tag{32}$$

Note that in contrast to the DTMC model, the CTMC model does not require the thresholds λ_1 and λ_2 to take specific values. λ_1 and λ_2 are computed using (20) based on the selected P_{nominal} and $P_{\max}$ values. More specifically, λ_1 is computed by setting $\left[\frac{C}{N}\right]$ in (20) to SINR$_{th}$ and $[P_T]$ to P_{nominal}, in dB. Then, the corresponding $[P_N]$ is the value of λ_1. Similarly, λ_2 is computed by setting $\left[\frac{C}{N}\right]$ to SINR$_{th}$ and $[P_T]$ to $P_{\max}$. The corresponding $[P_N]$ is the value of λ_2.

An alternative description of the above MC is to say that the time until the MC changes its state x is exponentially distributed with parameter $\rho(x)$ (i.e., if X_t represents the state of the MC at time t and $\tau \triangleq \inf\{t : X_t \neq x\}$, then $E[\tau] = 1/\rho(x)$), and the probability that the MC changes to y is $\alpha(x, y)/\rho(x)$. Let $\rho_{\max} \stackrel{\text{def}}{=} \max_{x \in \{1,2,3\}} \{\rho(x)\}$.

Finally, the stability condition introduced in Section 5.1, can be reformulated for the CTMC as follows. Assume that we are currently in slot n and we want to select a channel to be used after K time slots. Then, the stability condition for channel d_{n+K} is

$$q_z(i, i) + q_z(i, i-1) > p_{th} \tag{33}$$

where $z \stackrel{\text{def}}{=} KT + T_{data} - x\tau_s$.

7. OPTIMAL SENSING TIME

If the CR module cannot find a stable and usable channel to be used for transmission during a given slot n, we say that slot n is a *black hole* (BH). From Algorithm 1, as l increases, the probability of finding a usable and stable channel for a given slot increases, but at the same time $K = \lceil (l\tau_s + \tau_f)/T \rceil$ increases, which decreases the freshness of the sensed information and affects the probability of satisfying the stability condition. Our objective is to select the values of l and K such that the probability of a BH is minimized, subject to the constraint $KT < 1/\rho_{\max}$. This constraint ensures that the time between sensing a given channel and actually using it is less than the minimum expected time until the MC changes its state (i.e., $1/\rho_{\max}$, where $\rho_{\max}$ is defined in Section 6). Formally, the problem of selecting the optimal values of l and K can be stated as follows (note that the optimization problem is formulated for the CTMC model only):

DOI: 10.1002/sat

Problem 1:

$$\underset{l}{\text{minimize}}\ \Pr[\text{BH}] \tag{34}$$

$$\text{subject to: } KT < \frac{1}{\rho_{\max}}. \tag{35}$$

Let Ψ denote the set of channels that are either unusable or unstable. Then, $\Pr[\text{BH}]$ can be expressed as:

$$\Pr[\text{BH}] = \Pr\left[\bigcap_{i=0}^{l-1}(d_{n+K+i} \in \Psi)\right] = \Big(\Pr[d_{n+K} \in \Psi]\Big)^{l}. \tag{36}$$

In typical FH sequences, successive channels are sufficiently separated such that their states can be considered independent. For an arbitrary channel w, $\Pr[w \in \Psi]$ is given by:

$$\Pr[w \in \Psi] = \Pr[w \text{ is unusable}] + \Pr[w \text{ is unstable}]. \tag{37}$$

Note that $\Pr[w \text{ is unusable and unstable}] = 0$ because the stability criterion is defined only under states 1 and 2, and the only unusable state is state 3. Hence, $\Pr[w \text{ is unusable and unstable}] = \Pr[w \text{ is in state 3 and unstable}] = 0$.

Using Bayes' theorem,

$$\Pr[w \text{ is unstable}] = \Pr[w \text{ is unstable and in state 1}] + \Pr[w \text{ is unstable and in state 2}]. \tag{38}$$

Hence,

$$\Pr[w \in \Psi] = \pi_3 + \pi_1 \Pr[(p_z(1,2) + p_z(1,3)) \geq 1 - p_{th}] + \pi_2 \Pr[p_z(2,3) \geq 1 - p_{th}]. \tag{39}$$

From the analysis above, we conclude the following:

1. $\Pr[\text{BH}]$ is a function of A, z, and p_{th}.
2. $K = \lceil (l\tau_s + \tau_f)/T \rceil$ is a nondecreasing function of l for fixed values of τ_s, τ_f, and T. Hence, z is a nondecreasing function of l for fixed values of $\tau_s, \tau_f, T, T_{data}$, and x.
3. The behavior of $p_z(i,j)$ as l increases varies depending on A, which depends on λ_1 and λ_2 (recall from Section 6 that λ_1 and λ_2 are computed based on P_{nominal} and $P_{\max}$).

From point (3), it is difficult to obtain the optimal value of l that minimizes $\Pr[\text{BH}]$ for a general matrix A. Instead, for a given matrix A, we compute $\Pr[\text{BH}]$ for a range of values for l, between 1 and $l_{\max}$, and then select the value of l that minimizes $\Pr[\text{BH}]$. $l_{\max}$ is selected to satisfy the constraint in Problem 1, which can be expressed as follows:

$$\left\lfloor \frac{1}{T} \cdot \frac{1}{\rho_{\max}} \right\rfloor = \left\lceil \frac{l_{\max}\tau_s + \tau_f}{T} \right\rceil. \tag{40}$$

8. PERFORMANCE EVALUATION

In this section, we evaluate the performance of OSDFH via simulations and compare it with the conventional static FH approach. Our Matlab-based simulations are conducted for the DTMC and CTMC models. Our performance measures are the number of BHs and the number of transmission errors (TEs). A TE occurs when the estimated channel state is better than the actual state of that channel, encountered at the time of transmission. The concept of a BH is not applicable to the fixed FH design. Therefore, only the number of TEs is depicted for the fixed FH case. Unless stated otherwise, the default values of the simulation parameters for the DTMC and CTMC models are listed in Tables II and III, respectively. The transition probability matrix P (for the DTMC), the

DOI: 10.1002/sat

Table II. Simulation parameters for the DTMC model.

Parameter	Value
K	3 slots
l	4 slots
p_{th}	0.7
Length of the FH sequence	1000 slots

Table III. Simulation parameters for the CTMC model.

Parameter	Value
K	3 slots
l	4 slots
p_{th}	0.7
Length of the FH sequence	100 slots
τ_s	0.25 T
τ_f	1 T

Table IV. Example explaining the operation of OSDFH.

Time ($x\tau_s$)	Tx slot	Sensing slot	State of sensed Ch. (i)	$p^K_{i,i} + p^K_{i,i-1}$	Actual Ch. state
1	1	3	1	0.914	2
2	1	4	–	–	–
3	2	4	2	0.628	2
4	2	5	1	0.914	1
5	3	5	2	0.628	3
6	3	6	2	0.628	2
7	4	6	1	0.914	1
8	4	7	–	–	–
9	5	7	1	0.914	1
10	5	8	–	–	–

generator matrix A (for the CTMC), and the steady-state distribution π are given by:

$$P = \begin{pmatrix} 0.7 & 0.3 & 0 \\ 0.2 & 0.5 & 0.3 \\ 0 & 0.3 & 0.7 \end{pmatrix}$$

$$A = \begin{pmatrix} -3 & 3 & 0 \\ 1 & -3 & 2 \\ 0 & 3 & -3 \end{pmatrix}$$

$$\pi = \begin{pmatrix} 0.25 & 0.375 & 0.375 \end{pmatrix}.$$

8.1. Numerical Example

We first consider a simple numerical example, with the goal of explaining the operation of OSDFH. We assume the DTMC model. Consider the FH sequence in Figure 2, where K = 2 and l = 2. The transition matrix P is given above. For this numerical example, we ignore T_{data} and x in the stability definition of Section 5.1.

In the first transmission (Tx) slot and the first sensing duration ($x = 1$ in Table IV), the CR module senses channel d_3. Because d_3 is usable (in state 1) and also stable ($p^{(K)}_{i,i} + p^{(K)}_{i,i-1} = 2p^{(2)}_{1,1} = 0.914 > p_{th}$), the CR module assigns channel d_3 to slot 3. Assume that the actual channel state after $K = 2$ slots is 2, so a TE will occur because P_{nominal} is not enough to meet the required SINR at the receiver. (Recall from Section 5.4 that P_{nominal} meets the required SINR at the receiver when the channel is in state 1, i.e., when the received interference power is less than λ_1 dB). We continue in the same way

DOI: 10.1002/sat

for the remaining slots in Table IV. The resulting FH sequence after executing Algorithm 1 is as follows: $h_3 = d_3$ (TE), $h_4 = d_5$, $h_5 = \emptyset$ (BH), $h_6 = d_6$, and $h_7 = d_7$. In this example, the number of BHs equals 1 and the number of TEs equals 1.

8.2. DTMC Results

In this section, we study the effects of p_{th} and l on the numbers of BHs and TEs under the DTMC model. Recall from Section 5.1 that p_{th} represents the stability threshold, i.e., if with probability p_{th} the quality of the channel is not expected to deteriorate before completing the scheduled transmission, then this channel is considered stable. l is the maximum number of channels that can be sensed during one slot.

8.2.1. Number of BHs

Figures 5(a) and (b) show the number of BHs as a function of p_{th} and l, respectively. The number of BHs increases significantly when p_{th} exceeds 0.6, reaching its maximum value of 1000 when $p_{th} = 0.7$. As can be observed in Figure 5(b), increasing l beyond 3 does not affect the number of BHs when $p_{th} = 0.7$. When $p_{th} = 0.5$, increasing l beyond 2 reduces the number of BHs significantly, as the CR module has a higher chance of finding a channel when the number of sensing periods increases (as long as p_{th} is not too large).

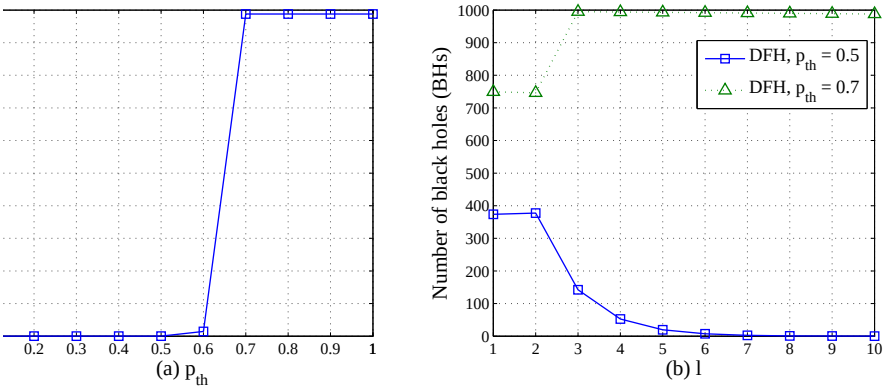

Figure 5. Number of BHs versus (a) p_{th}, and (b) l under the DTMC model.

8.2.2. Number of TEs

Figures 6(a) and (b) depict the number of TEs as a function of p_{th} and l, respectively. The number of TEs decreases significantly when p_{th} exceeds 0.5, and reaches its minimum value of 0 at $p_{th} = 0.7$. Even when p_{th} is small, the proposed DFH approach achieves a significantly smaller number of TEs than the conventional FH approach. As Figure 6(b) shows, for reasonably large values of l, the number of TEs becomes insensitive to l. Hence, as long as l is large enough, the number of TEs mainly depends on p_{th}. For $p_{th} = 0.5$ in Figure 6(b), the number of TEs is large because the probability that the channel stays in the same state is small, and for $p_{th} = 0.7$, the number of TEs is small because this probability is high. The number of TEs for the conventional FH scheme does not depend on p_{th} or l because this scheme uses a fixed FH pattern. The small fluctuation in the figure is due to the randomness in the channel state. The plotted values in the figure are averaged over a sufficiently large number of runs.

8.3. CTMC Results

In this section, we study the effects of p_{th} and l on the numbers of BHs and TEs under the CTMC model. Recall that the value of l under this model is obtained from Section 7.

DOI: 10.1002/sat

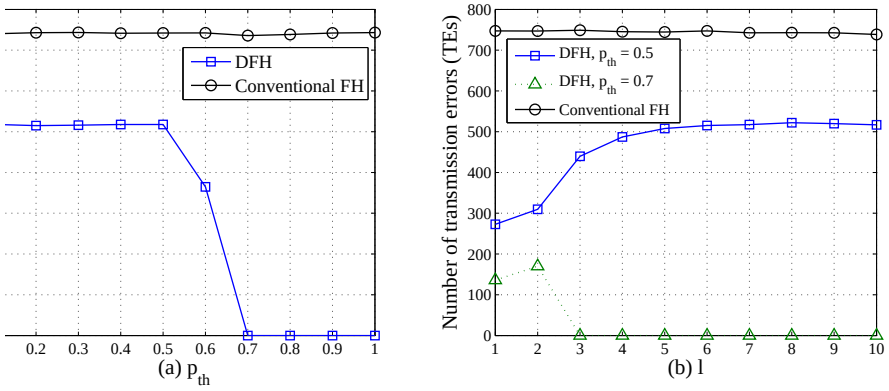

Figure 6. Number of TEs versus (a) p_{th}, and (b) l under the DTMC model.

8.3.1. Effect of p_{th} on the Number of BHs and TEs

Figure 7 shows the number of BHs and TEs as a function of p_{th}. The number of BHs increases significantly when p_{th} exceeds a critical value, say $c_{BH} = 0.6$, reaching its maximum value of almost 100 when $p_{th} = 0.7$ (which is inline with the DTMC results). By increasing p_{th}, the chances of satisfying the stability condition decrease, and hence the number of BHs increases. The number of TEs decreases significantly when p_{th} exceeds $c_{TE} = 0.6$ and reaches its minimum value of almost 0 at $p_{th} = 0.7$ (which is also consistent with the results of the DTMC model). As shown in the figure, the conventional FH scheme results in much higher TEs than the DFH scheme, even when p_{th} is very small. As p_{th} decreases, the stability requirement becomes less stringent, and the accuracy of the sensed channel interference decreases. This results in an increase in the number of TEs. c_{BH} and c_{TE} depend on the transition rates of the system, which depend on λ_1 and λ_2.

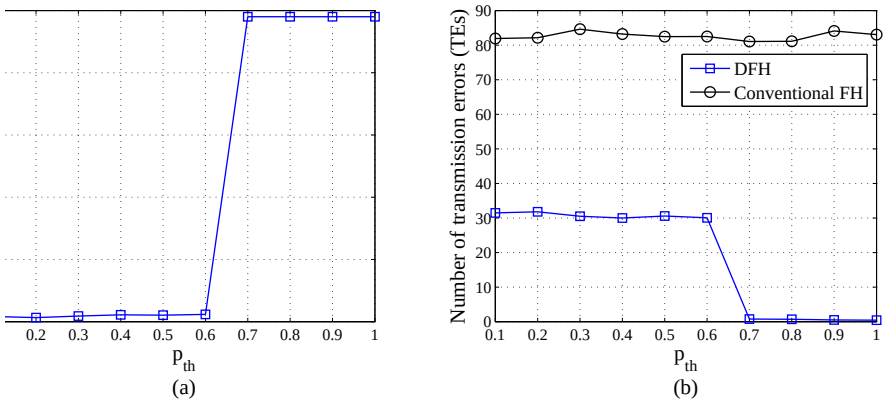

Figure 7. Number of (a) BHs and (b) TEs versus p_{th} under the CTMC model.

8.3.2. Effect of l on the Number of BHs and TEs

The effect of l on the numbers of BHs and TEs depends on p_{th} and the transition rates of the system. Figure 8 depicts the performance as a function of l. For $p_{th} = 0.5$, increasing l has barely any impact on the number of BHs, whereas for $p_{th} = 0.8$ and $p_{th} = 1$, the number of BHs decreases as l increases. Similarly, for $p_{th} = 0.5$, increasing l has almost no effect on the number of TEs, whereas for $p_{th} = 0.8$ and $p_{th} = 1$, the number of TEs increases with l. As mentioned before, the performance of the conventional FH scheme is not affected by p_{th} or l.

DOI: 10.1002/sat

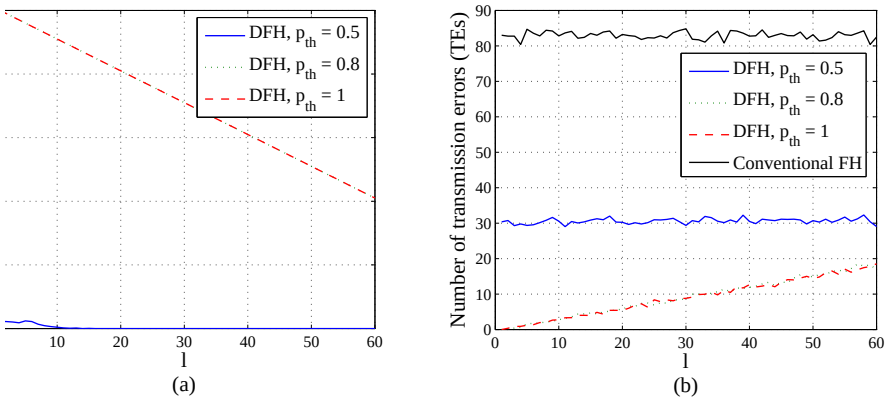

Figure 8. Number of (a) BHs and (b) TEs versus l under the CTMC model.

9. CONCLUSIONS

In this paper, we used proactive detection of RF interference to adjust in real-time the hopping sequence for communications over a satellite link. Our proposed OSDFH protocol exploits the sensing capabilities of a CR for proactive detection of channel quality. We analyzed the design parameters of our protocol using DTMC and CTMC models. We proposed an algorithm for searching for a usable and stable channel, and for adjusting the FH sequence based on channel quality and stability. Using simulations, we studied the effects of different system parameters on performance. The DTMC and CTMC models produced consistent results.

REFERENCES

1. Lightfoot L, Zhang L, Li T. Space-time coded collision-free frequency hopping in hostile jamming. *Proceedings of the IEEE Military Communications Conference* November 2008; pp. 1-7, DOI: 10.1109/MILCOM.2008.4753220.
2. Lockheed Martin Space Systems Company. Advanced EHF: Assured, Protected, Survivable. url: http://www.lockheedmartin.com/content/dam/lockheed/data/space/documents/AEHF/C10010_AEHFFactsheet_V282911.pdf.
3. Northrop Grumman Corporation. Milstar Payloads. url: http://www.northropgrumman.com/Capabilities/MilstarPayloads/Pages/default.aspx.
4. National Aeronautics and Space Administration. Space Network User's Guide (SNUG). August 2007.
5. Harrison T. The future of MILSATCOM. *Center for Strategic and Budgetary Assessments*.
6. Hu W, Willkomm D, Abusubaih M, Gross J, Vlantis G, Gerla M, Wolisz A. Cognitive radios for dynamic spectrum access - dynamic frequency hopping communities for efficient IEEE 802.22 operation. *IEEE Communications Magazine* May 2007; **45(5)**, pp. 80-87, DOI: 10.1109/MCOM.2007.358853.
7. Tong J, Wu H, Yin C, Ma Y, Li J. Dynamic frequency hopping vs. non-hopping in IEEE 802.22 systems. *Proceedings of the IEEE IC-NIDC Conference* November 2009; pp. 95-99, DOI: 10.1109/ICNIDC.2009.5360992.
8. Jembre YZ, Choi Y-J, Pak W. Out-of-band sensing for seamless communication in cognitive radio systems. *Proceedings of the CUTE Conference* Decemeber 2010; pp. 1-4, DOI: 10.1109/ICUT.2010.5677673.
9. Kang B-J, Park H-S, Kim Y-S, Woo S-M, Ban S-W. Out-of-band cooperative spectrum sensing in cognitive radio system of multiple spectrum bands. *Proceedings of the WSEAS Conference* 2009; pp. 31-34.
10. Sharma SK, Chatzinotas S, Ottersten B. Satellite cognitive communications: Interference modeling and techniques selection. *Proceedings of the Advanced Satellite Multimedia Systems (ASMS) Conference and Signal Processing for Space Communications (SPSC) Workshop* 2012; pp. 111-118, DOI: 10.1109/ASMS-SPSC.2012.6333061.
11. Sharma SK, Chatzinotas S, Ottersten B. Spectrum sensing in dual polarized fading channels for cognitive SatComs. *Proceedings of the IEEE GLOBECOM Conference* 2012; pp. 3419-3424, DOI: 10.1109/GLOCOM.2012.6503643.
12. Yun YH, Cho JH. An orthogonal cognitive radio for a satellite communication link. *Proceedings of the IEEE International Symposium on Personal, Indoor and Mobile Radio Communications* 2009; pp. 3154-3158, DOI: 10.1109/PIMRC.2009.5449826.
13. Kandeepan S, De Nardis L, Di Benedetto M-G, Guidotti A, Corazza GE. Cognitive satellite terrestrial radios. *Proceedings of the IEEE GLOBECOM Conference* 2010; pp. 1-6, DOI: 10.1109/GLOCOM.2010.5683428.
14. Australian Communications Authority. Little LEO satellite systems: Potential for interference to earth station receivers in the band 137-138 MHz. url: http://www.acma.gov.au/webwr/radcomm/frequency$planning/spps/9705spp.pdf$.
15. Fossa CE, Raines RA, Gunsch GH, Temple MA. An overview of the IRIDIUM low earth orbit (LEO) satellite system. *Proceedings of the IEEE National Aerospace and Electronics Conference (NAECON)* 1998; pp. 152-159, DOI:

10.1109/NAECON.1998.710110.
16. Maine K, Devieux C, Swan P. Overview of IRIDIUM satellite network. *Proccedings of the IEEE WESCON Conference* 1995; pp. 483-490, DOI: 10.1109/WESCON.1995.485428.
17. Qualcomm Announces Sampling of the Industry's First Single-Chip Receive Diversity Device for Increased CDMA2000 Network Capacity. url: http://www.qualcomm.com/press/releases/2005/050504-rfr6500.html.
18. Kenwood TH-D7A dual-band handheld transceiver. url: http://www.kenwoodusa.com/Communications/AmateurRadio/Portables/TH-D7A(G).
19. Digham FF, Alouini M-S, Simon MK. On the energy detection of unknown signals over fading channels. *Proceedings of the IEEE ICC Conference* May 2003; pp. 3575-3579. DOI: 10.1109/ICC.2003.1204119.
20. Babich F, Lombardi G, Valentinuzzi E. Variable order Markov modelling for LEO mobile satellite channels. *Electronics Letters* April 1999; **35(8)**, pp. 621-623, DOI: 10.1049/el:19990455.
21. Beaulieu NC, Dong X. Level crossing rate and average fade duration of MRC and EGC diversity in Ricean fading. *IEEE Transactions on Communications* May 2003; **51(5)**, pp. 722-726, DOI: 10.1109/TCOMM.2003.811380.
22. Bhaskar V. Finite-state Markov model for Lognormal, Chi-square (central), Chi-square (non-central), and K-distributions. *International Journal of Wireless Information Networks* 2007; **14**, pp. 237-250, DOI: 10.1007/s10776-007-0065-2.
23. Proakis JG. Digital Communications. McGraw Hill, 2001.
24. Davis LM, Collings IB, Evans RJ. Estimation of LEO satellite channels. *Proceedings of the International Conference on Information, Communications and Signal Processing (ICICS)* 1997; **1**, pp. 15-19, DOI: 10.1109/ICICS.1997.647048.
25. Wang HS, Moayeri N. Finite-state Markov channel-a useful model for radio communication channels. *IEEE Transactions on Vehicular Technology* February 1995; **44(1)**, pp. 163-171, DOI: 10.1109/25.350282.
26. Zhang Q, Kassam SA. Finite-state Markov model for Rayleigh fading channels. *IEEE Transactions on Communications* Novemeber 1999; **47(11)**, pp. 1688-1692, DOI: 10.1109/26.803503.
27. Roddy D. Satellite communications. McGraw-Hill, 2006.
28. Lawler GF. Introduction to stochastic processes. Chapman and Hall/CRC, Taylor and Francis Group, 2006.
29. Zorzi M, Rao RR. On the statistics of block errors in bursty channels. *IEEE Transactions on Communications* June 1997; **45(6)**, pp. 660-667. DOI: 10.1109/26.592604.
30. Rappaport TS. Wireless communications: principles and practice. Prentice Hall, 2001.
31. Iskander C-D, Mathiopoulos PT. Analytical level crossing rates and average fade durations for diversity techniques in Nakagami fading channels. *IEEE Transactions on Communications* August 2002; **50(8)**, pp. 1301-1309, DOI: 10.1109/TCOMM.2002.801465.
32. Turin W, Nobelen RV. Hidden Markov modeling of flat fading channels. *IEEE Journal on Selected Areas in Communications* 1998; **16(9)**, pp. 1809-1817. DOI: 10.1109/49.737649.

AUTHOR'S BIOGRAPHIES

Mohammad J. Abdel-Rahman received the M.S. degree in electrical engineering from Jordan University of Science and Technology (JUST), Jordan, in 2010 and the B.S. degree in communication engineering from Yarmouk University, Jordan, in 2008. He is currently working toward the Ph.D. degree in electrical and computer engineering at the University of Arizona, where he is a research assistant in the advanced networking lab. His current research interests are in wireless communications and wireless networking, with emphasis on wireless cognitive radio networks. He has published several papers in international conferences and journals. He serves as a reviewer for several international conferences and journals. He is a member of the IEEE.

Prepared using satauth.cls
DOI: 10.1002/sat

Marwan Krunz received the PhD degree in electrical engineering from Michigan State University in 1995. He has been with the University of Arizona since 1997, where he is a professor in the Electrical and Computer Engineering and Computer Science Departments. He is the UA site director for Connection One. He has held several visiting research positions and was a Chair of Excellence at the University of Carlos III, Madrid, Spain. His research interests include computer networking and wireless communications with a focus on distributed radio resource management in wireless and sensor networks, protocol design, and secure communications. He has published more than 170 journal articles and refereed conference papers and is a coinventor on three US patents. He was a recipient of the US National Science Foundation (NSF) CAREER Award in 1998. He has served on the editorial boards for the IEEE Transactions on Network and Service Management, IEEE/ACM Transactions on Networking, IEEE Transactions on Mobile Computing, and Computer Communications Journal, and as a TPC chair for several international conferences. He is a fellow of the IEEE.

R. Scott Erwin received a B. S. in Aeronautical Engineering from Rensselaer Polytechnic Institute in 1991, and the M. S. and Ph.D. degrees in Aerospace Engineering from the University of Michigan in 1993 and 1997, respectively. He has been an employee of the Air Force Research Laboratory, Space Vehicles Directorate (AFRL/RV) located at Kirtland AFB, NM, from 1997 to the present. He is currently a Principal Research Aerospace Engineer and the Guidance, Navigation, & Control (GN&C) Program Manager. His responsibilities include both performing and managing basic and applied research in space communications systems, spacecraft control and, and satellite autonomy. He is the author or co-author of over sixty technical publications in the areas of spacecraft communications, dynamics & controls. His current research interests are autonomous spacecraft, satellite communications, and the interplay between communications, estimation, and control in networked space systems. He is an Associate Fellow of AIAA and a Senior Member of IEEE.

DOI: 10.1002/sat